ELSEVIER

European Journal of Cancer 40 (2004) 1082–1094

European Journal of Cancer

www.ejconline.com

Distinct patterns of genetic alterations in adenocarcinoma and squamous cell carcinoma of the lung

S.M.-H. Sy[a], N. Wong[a,*], T.-W. Lee[b], G. Tse[c], T.S.-K. Mok[a], B. Fan[a], E. Pang[a], P.J. Johnson[d], A. Yim[b]

[a]*Department of Clinical Oncology, Sir Y.K. Pao Centre for Cancer, The Chinese University of Hong Kong, Shatin, SAR Hong Kong, China*
[b]*Department of Surgery, Sir Y.K. Pao Centre for Cancer, The Chinese University of Hong Kong, Shatin, SAR Hong Kong, China*
[c]*Department of Anatomical and Cellular Pathology, Sir Y.K. Pao Centre for Cancer, The Chinese University of Hong Kong, Shatin, SAR Hong Kong, China*
[d]*Department of Oncology and Translational Research, University of Birmingham, UK*

Received 28 October 2003; received in revised form 12 January 2004; accepted 15 January 2004

Abstract

Squamous cell carcinoma (SqC) and adenocarcinoma (AdC) are the two most common subtypes of non-small cell lung cancer (NSCLC). Cumulative information suggests that the SqC and AdC subtypes progress through different carcinogenic pathways, but the genetic aberrations promoting such differences remain unclear. Here we have assessed the overall genomic imbalances and structural abnormalities in SqC and AdC . By parallel analyses with comparative genomic hybridisation (CGH) on tumorous lung tissues and spectral karyotyping (SKY) on short-term cultured primary tumours, genome-wide characterisation was carried out on 69 NSCLC (35 SqC, 34 AdC). Molecular cytogenetic characterisation indicated common and distinct genetic changes in SqC and AdC. Common events of +1q21-q24, +5p15-p14, and +8q22-q24.1, and −17p13-p12 were found in both groups, although hierarchical clustering simulation on CGH findings depicted +2p13-p11.2, +3q25-q29, +9q13-q34, +12p, +12q12-q15 and +17q21, and −8p in preferential association with SqC pathogenesis ($P<0.05$). Corresponding SKY analysis suggested that these changes occur in simple and complex rearrangements, and further indicated the clonal presence of translocation partners leading to chromosomal over-representations. These recurring rearrangements involved chromosome pairs of t(1;13), t(1;15), t(7;8), t(8;15), t(8;9), t(2;17) and t(15;20). Of particular interest was the finding that the t(8;12) translocation partner was exclusive to AdC. The combined application of SKY and CGH has thus uncovered the genome-wide chromosomal aberrations in NSCLC. Specific chromosomal imbalances and translocation partners found in SqC and AdC have highlighted regions for further molecular investigation into gene(s) that may hold importance in the carcinogenesis of NSCLC.

Keywords: NSCLC; Comparative genomic hybridisation; Spectral karyotyping

1. Introduction

Lung cancer is responsible for the highest cancer-related morbidity and mortality worldwide [1]. Non-small cell lung cancer (NSCLC) comprises approximately 80% of all lung cancers, among which adenocarcinoma (AdC) and squamous cell carcinoma (SqC) are now the two most common histological subtypes. Cigarette smoking continues to be an important aetiological factor, with a clear implication of involvement in over 95% of male cases [2]. A correlation between the incidence of lung cancer in females and smoking habit has also been observed in recent years [3].

Due to the high incidence and mortality rates, much effort has been drawn towards investigating the cause and course of NSCLC. Although classical cytogenetic studies by banding analysis can provide an overall view of structural and numerical abnormalities, the frequent presence of karyotypic complexity has precluded more accurate interpretation. Conversely, molecular characterisation by comparative genomic hybridisation (CGH) and allelotyping has shown common over-

* Corresponding author. Department of Clinical Oncology, The Chinese University of Hong Kong, Prince of Wales Hospital, Shatin, N. T., SAR Hong Kong, China. Tel.: +852-2632-1128; fax: +852-2648-8842.
E-mail address: natwong@cuhk.edu.hk (N. Wong).

0959-8049/$ - see front matter © 2004 Elsevier Ltd. All rights reserved.
doi:10.1016/j.ejca.2004.01.012

representations of 1q, 3q, 5p, 8q and 20, and loss of heterozygosity (LOH) on 3p, 8p, 13q and 17p in NSCLC [4–6]. Despite the reportedly frequent genomic imbalances, the pattern of karyotypic alterations associated with AdC and SqC remains uncertain.

We have now conducted a comprehensive molecular cytogenetic characterisation of AdC and SqC tumours. By utilising CGH findings as a frame, individual information was examined in relation to chromosomal rearrangements described from spectral karyotyping (SKY). Cytogenetic information on NSCLC has mainly been derived from cell lines [7,8], and we believe our study is the first to describe such information in primary tumours. Our combined CGH and SKY analysis shows distinct patterns of genetic aberration in the two specific NSCLC subtypes, which might in turn influence the different pathogenetic pathways adopted by these tumours.

2. Materials and methods

2.1. Patients

Tumorous lung tissues were collected from 69 patients who underwent curative surgery for lung cancer at the Prince of Wales Hospital, Hong Kong. Tumours were classified according to the World Health Organisation histological typing of lung tumours, and staged according to the TNM classification of malignant tumours. 34 cases were diagnosed as AdC (age 43–79 years; stage $T_{1-4}N_{0-2}M_{0-1}$) and 35 cases as SqC (age 47–83 years; stage $T_{1-4}N_{0-2}M_0$). All patients had a smoking history. A smoker was defined as a patient who had been consuming tobacco for more than 5 years and had smoked up to the time of diagnosis. The clinicopathological characteristics of the patients are shown in Table 1. Our AdC and SqC groups were not statistically different in terms of age, sex or TNM stages ($P > 0.05$).

Surgical lung tissues were transported in medium to the laboratory within 1 h of operation. A portion of the tumour tissue was subjected to short-term cell culture and subsequent SKY analysis; DNA was extracted from the remainder for parallel CGH studies. Histological examination was performed before the CGH analysis to confirm the suitability of tumour cell content (>70%). In cases with suboptimal content, the tissue was microdissected under the guidance of an experienced lung pathologist (G.T.) to enrich the percentage cell recovery.

2.2. Comparative genomic hybridisation

The CGH protocol was according to the method of Kallioniemi and colleagues [9] with modifications described in [10]. In brief, differentially labelled tumour and reference DNAs with biotin-16-dUTP and digoxigenin (dig)-11-dUTP (Boehringer Mannheim, Mannheim, Germany), respectively, were hybridised on to normal metaphase chromosomes. Following hybridisation, biotin signals were detected with conjugated avidin-fluorescein isothiocyanate antibody (Sigma, St. Louis, USA) and dig-labelled DNA was visualised by tetramethylrhodamine isothiocyanate-conjugated antibody (Sigma). Metaphase chromosomes counterstained with 4′,6-diamidino-2-phenylindole (DAPI) were captured through a cooled CCD camera mounted on a Leitz DMRB fluorescence microscope (Leica, Wetzlar, Germany) and the hybridised signals were analysed with CGH software version 3.1 on *Cytovision* (Applied Imaging Ltd., Sunderland, UK). The average ratio profile on each chromosome was calculated, based on the analysis of 8-12 metaphases. Thresholds for gains and losses were defined as the theoretical values of 1.25 and 0.75, respectively, and amplifications were considered when the ratios exceeded 1.5 [11,12].

CGH findings were further simulated by hierarchical clustering (http://genome-www.stanford.edu/) [13]. CGH interpretations were first recoded before clustering analysis. In each case, any CGH alterations identified were recoded into continuous numbers by $y = ((x-1)/0.25) + 1$, where x was the mean of the test:reference ratio. For example, chromosome region A with a test:reference ratio of 1.5 would be assigned "3", based on $x = 1.5$ and $y = ((1.5-1)/0.25) + 1$. Accordingly, chromosomal regions displaying copy loss,

Table 1
Clinicopathological features of the patients with non-small cell lung cancer (NSCLC)

	NSCLC		
	Squamous cell carcinoma	Adenocarcinoma	*P*
Age (years)			
Range	47–83	43–79	0.692
Sex			
Male	34 (97.1%)	31 (91.2%)	0.356
Female	1 (2.9%)	3 (8.8%)	
T values			
T_1	7 (20.0%)	4 (11.8%)	0.187
T_2	22 (62.9%)	26 (76.5%)	
T_3	5 (14.3%)	1 (2.9%)	
T_4	1 (2.9%)	3 (8.8%)	
Lymph node involvement			
N_0	23 (65.7%)	23 (67.6%)	0.345
N_1	9 (25.7%)	5 (14.7%)	
N_2	3 (8.6%)	6 (17.6%)	
Metastatic behaviour			
M_0	35 (100.0%)	32 (94.1%)	0.239
M_1	0 (0.0%)	2 (5.9%)	

a balanced profile, copy gain and regional amplification were assigned 0, 1, 2 and 3, respectively. Clustered patterns were presented graphically using *Treeview* (http://genome-www.stanford.edu/) [13].

2.3. Cell culture

Tumorous lung tissues were short-term cultured according to the method described in [14]. Tumour tissue was finely minced with sterile scalpels and digested with collagenase type II (200 U/ml) for 1–2 h at 37 °C, depending on the consistency of the tissue. Desegregated cell suspension was seeded in RPMI 1640 Glutamax medium with HEPES buffer supplemented with 16% fetal bovine serum, 35 U/ml penicillin, 35 μg/ml streptomycin, 10 ng/ml selenium, 10 μg/ml transferrin and 10 μg/ml insulin. Culture time depended on cell proliferation. At 80% confluence, which took on average 7–10 days, cells were harvested for metaphase by colchicine.

2.4. Spectral karyotyping

The SKY analysis was carried out according to the method described by Schröck and colleagues [15] with modifications as described in [14]. Metaphase spreads prepared from short-term cultured, primary NSCLC were denatured in 70% formamide/2× sodium saline citrate (pH 7.0). SkyPaint™ probe (Applied Spectral Imaging, Migdal Haemek, Israel) was hybridised on to the denatured metaphases in dark humid chambers at 37 °C for 48 h. After post-hybridisation washes, the biotinylated probes were visualised using avidin Cy5, and the dig-labelled probes by antimouse antibody followed by goat antimouse Cy5.5 conjugate.

Images of DAPI-counterstained chromosomes were acquired with an SD200 Spectracube (Applied Spectral Imaging) mounted on a Leica DMRXA microscope (Leica) through a custom-designed optical SKY-1 filter. Spectral information obtained on each chromosome was analysed with *SkyView 1.61* software (Applied Spectral Imaging). Karyotypical interpretations were according to the ISCN nomenclature 1995 [16]. A translocation event was considered recurrent when observed in two or more cases, and a similar breakpoint involved in one or more alterations within the same case was counted as occurring once.

2.5. Statistical analysis

Clinicopathological features of AdC and SqC patients were compared by the Mann–Whitney test and Pearson's χ^2 test. The average copy-number aberrations, whether gains or losses, were compared by Student *t*-test. All statistical analyses were done with *SPSS for Windows 10.0* software (SPSS Inc., Chicago).

3. Results and discussion

CGH analysis of 69 NSCLC specimens produced informative findings in 61 (88%). In the series of SqC and AdC examined, genomic gains prevailed over losses ($P<0.0005$): a ratio of 10.1 ± 5.6 copy gains $\pm$(mean + S.D.) to 4.9 ± 4.1 losses $\pm$occurred in SqC, and a ratio of 6.2 ± 5.1 copy gains $\pm$to 2.2 ± 1.8 losses in AdC. The aberrant tumour metaphases derived from SqC and AdC displayed a karyotype ranging from hyperdiploid to hypotetraploid. There was no significant difference in ploidy status between SqC and AdC ($P>0.05$), but despite similarities in their ploidy, a comparison of structural anomalies from SKY suggested a generally more disrupted genome in SqC than in AdC. A higher incidence of translocation events was found in SqC, in which there was an average 13.9 translocations per tumour as compared to 6.8 translocations per tumour in the AdC series. This difference also corresponded to higher average copy-number aberrations per tumour on CGH examination: 15.0 ± 9.0 aberrations per tumour in the SqC group $\pm$and 8.02 ± 5.5 in the AdC $\pm$($P=0.001$).

Although a more profound degree of chromosomal instability was evident in SqC, several genetic changes were nonetheless common in both subtypes. Regional

Table 2
Genomic imbalances in non-small cell lung cancers

Regions	Squamous cell carcinoma (%)	Adenocarcinoma (%)	*P*
Gains			
1q21-q24	42.86	42.42	0.973
2p13-p11.2	39.29	3.03	**0.001**
3q25-q29	85.71	21.21	**<0.0005**
5p15.3-p14	53.57	42.42	0.385
6p21.2-p12	35.71	12.12	**0.037**
7p22-p11.2	35.71	39.39	0.768
7q	42.86	30.30	0.281
8q22-q24.1	42.86	51.52	0.500
9q13-q34	32.14	3.03	**<0.0005**
11q12-q13	35.71	15.15	0.079
12p	46.43	18.18	**0.018**
12q13-q21	46.43	21.21	**0.018**
14q13-q22	17.86	30.30	0.373
17q21	53.57	21.21	**0.009**
20q11.2-q12	39.29	18.18	0.067
Xq13-q28	35.71	39.39	0.768
Losses			
3p	25.00	3.03	**0.019**
4q31.1-q35	28.57	6.06	**0.034**
8p23	42.86	15.15	**0.023**
9p23-p22	28.57	6.06	**0.034**
13q21	28.57	3.03	**0.009**
17p13-p12	28.57	33.33	0.689

Common aberrations only are listed. Statistical correlations between aberrations depicted by comparative genomic hybridizisation revealed significant differences in a number of regions between the two tumour types. *P*-values < 0.05 are shown in bold type.

gains on 1q (42–43%), 5p (40–52%), 8q (45–47%), and loss of 17p (25–35%), were frequent in both SqC and AdC ($P > 0.05$) (Table 2). While the observed common isochromosome formation of i(1)(q10), i(8)(q10) and i(17)(q10) might have highlighted the manifestation of whole-arm gains,preferential involvement of common SORs 1q21-q24, 5p15-p14, 8q22-q24 in complex rearrangements was also shown by the SKY analysis.

Our finding of non-random alterations in several chromosomal regions may have implications for genes residing at these sites, such as *hTERT* on 5p15, c-*myc* on 8q24 and the tumour-suppressor *TP53* on 17p13, in the development of the two common NSCLC subtypes. Amplification of *c-myc* may be correlated with lymph node metastasis in lung cancer [17] and may promote tumour formation via the induction of telomerase

Fig. 1. Simulation of findings from comparative genomic hybridisation of non-small cell lung cancer by hierarchical clustering. Cluster dendrogram showed two major branches that signify patterns of genetic alteration associated with squamous cell carcinoma (SqC) and adenocarcinoma (AdC). Colour bands red and green depicted under the cluster trees denote the majority of cases as SqC (83%) and AdC (82%), respectively. A subset of AdC patients (80%) with common Xq13-q28 copy-number gain clusters under the SqC branch (depicted by the pink band). Copy-number gain(s) and loss(es) are visualised in red and green, respectively, while black represents balanced copy number. Chromosomal regions that signify major differentiation between SqC and AdC are illustrated.

activity [18]. Ectopic expression of *hTERT* can direct tumour cells through crisis [19,20] and is a useful indicator for the prognosis of lung cancer [21]. A significantly higher plasma free-circulating DNA, detected by real-time PCR amplification of the *hTERT locus*, was found in NSCLC patients than controls [22]. LOH at *TP53* region has been described in NSCLC [23] and the frequent p53 mutations found in lung cancer patients might be directly related to DNA damage from tobacco carcinogens [24]. The role of *TP53* in smoking-related carcinogenesis is further demonstrated by the significant increase in lung tumour incidence in the dominant-negative *TP53* transgenic mouse following exposure to environmental cigarette smoke [25].

3.1. Patterns of genetic alterations

AdC and SqC differ in their locations, cell morphology and growth patterns. It is therefore likely that specific alterations are involved in their pathogenesis.

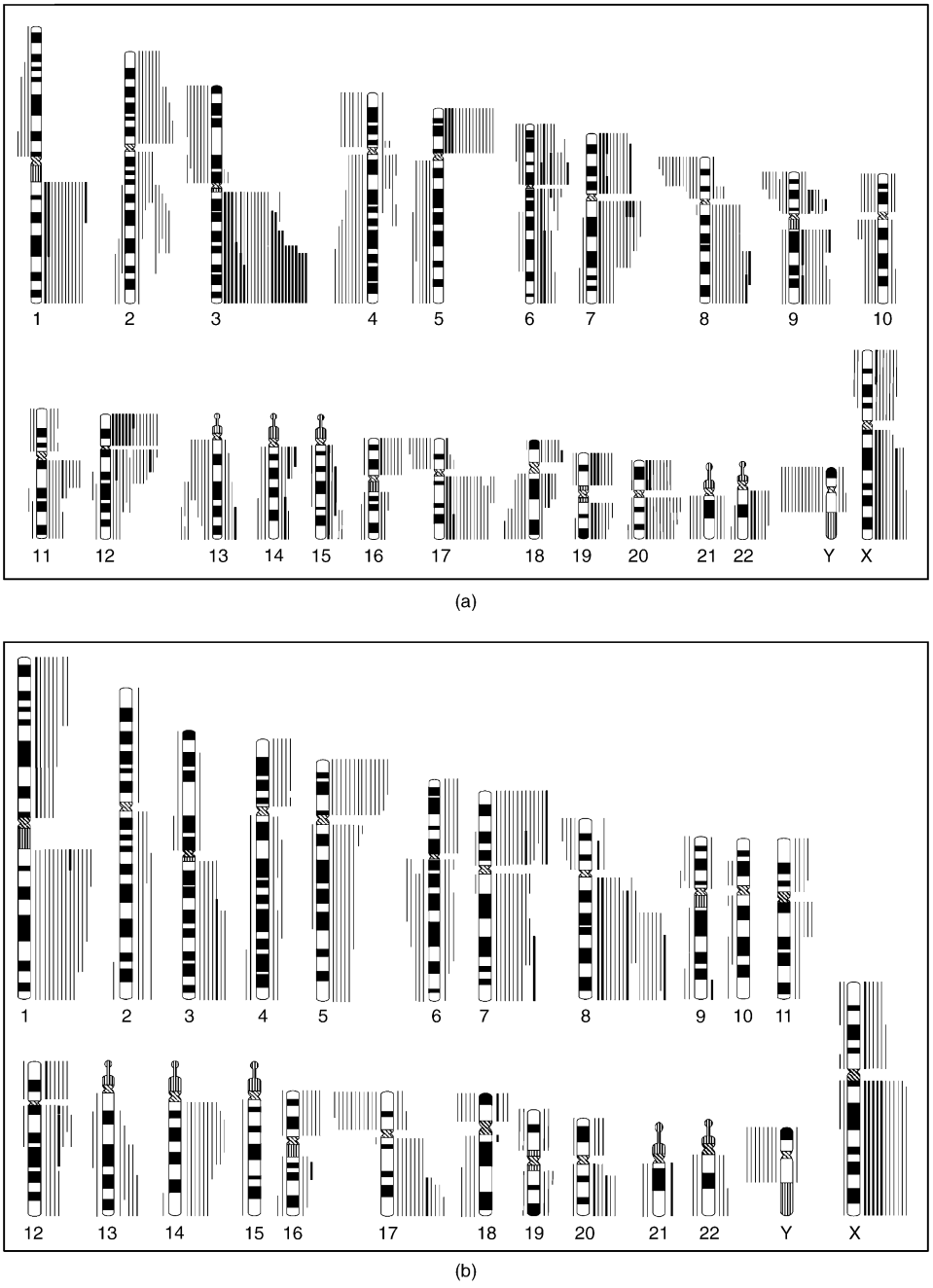

Fig. 2. Summary of comparative genomic hybridisation abnormalities identified in non-small cell lung carcinoma. Genetic changes detected in (a) squamous cell carcinoma and (b) adenocarcinoma. Each vertical line represents a single genetic aberration observed in a single tumour specimen. Losses are shown on left and gains on the right of individual chromosomes. High-level amplifications are shown as thick lines.

Table 3
SKY analysis on short-term cultured non-small cell lung cancer

Patient	Sex/age	TNM staging	Ploidy status	Clonal rearrangements
SqC-001	M/66	$T_2N_0M_0$	2n	der(3)t(3;19)(?;?)
SqC-002	M/61	$T_3N_1M_0$	2n	der(X)t(X;16)(q26;?) der(1)t(1;12)(p32;q21) ins(1;15)(q22;?) der(1)t(1;17)(q22;q11.1) dup(2)(p11.2pter) der(2;14)(p10;q10) der(2)t(2;17)(q21;q11.1) i(3)(q24q29) t(4;13)(q26;q33) der(7)t(7;16)(q10;q12.1) der(7)t(7;17)(q10;?) i(8)(q10) der(8;13)(q10;q10) der(9;20)(q10;q10) dup(10)(q10) dup(12)(q11q22) der(12;15)(q10;q10) der(14)t(3;14;1)(3?::14q10->q32::1p36.3->p13) der(21;22)(q10;q10) der(?)t(7;14)(?;?) der(?)t(8;15)(?;?) der(?)t(12;19)(?;?) der(?)t(12;17)(?;?) der(?)t(15;17)(?;?) der(?)t(15;19)(?;?) der(?)t(15;20)(?;?)
SqC-003	M/79	$T_1N_1M_0$	2n	der(1)t(1;7)(q32;q32) der(1)t(1;20)(q32;p12) der(?)t(1;21)(?;p?) der(?)t(2;12)(?;?)
SqC-004	M/62	$T_2N_0M_0$	2n	der(1)t(1;2)(?;?) der(1)t(1;5)(p13;?p11.2) der(1)t(1;?)(q21;?) der(3;14)(q10;q10) der(4)t(4;15)(?q28;?) der(8)t(8;9)(p12;q13) der(12)t(12;20)(q21;?) der(17)t(5;17)(p12;q10) der(21)t(20;21)(q11.2;q21)
SqC-005	M/50	$T_2N_1M_0$	2n	Normal karyotype
SqC-008	M/78	$T_2N_0M_0$	2n	Normal karyotype
SqC-009	M/71	$T_2N_0M_0$	3n	der(X)t(X;17)(q?;p?) der(1;9)(q10;q10) der(1;16)(q10;q10) der(2)t(2;17)(?;?) der(5)t(5;10)(?;?) der(20)t(12;20)(p10;?) t(7;8)(q21;?) der(7)t(7;8;?)(7q10->q36::8q?::?) der(11)t(11;20)(?;?) der(12)t(1;12)(?;p11) der(18)t(8;18)(?;?) der(18)t(18;20)(p11.2;?)
SqC-010	M/72	$T_3N_0M_0$	3n	der(7)t(19;7;17)(19?::7p22->q31::17q21->q25) der(8;13)(q10;q10) der(12)t(12;15)(q24.1;q14) der(15;18)(q10;q10)

(*continued on next page*)

Table 3 (*continued*)

Patient	Sex/age	TNM staging	Ploidy status	Clonal rearrangements
				der(19)t(3;19)(?;p11) der(20)t(9;20)(q13;q10) der(?)t(1;4)(?;?) der(?)t(8;9)(?;?)
SqC-011	M/74	$T_1N_0M_0$	2n	Normal karyotype
SqC-012	M/82	$T_3N_0M_0$	4n	der(X)t(X;18;10)(X?::18?::10?) der(Y)t(Y;11;15)(Yp11.3->q12::11?::15?) der(Y)t(Y;15)(q11;q26) i(1)(p10) der(1)t(1;?)(?;?) dic(1;19)(p13;p10) i(2)(p10) der(2;20)(p10;p10) der(3)t(3;15;3)(3p26->p10::15q11.1->q22::3q15->q29) der(3)t(3;9;15)(3p26->p14::9q11->q34:: 15?q22->q29) der(7;8)(p10;q10) der(7)t(7;16)(q11.2;?) der(7)t(7;18)(q11.2;q11.2) der(8)t(7;8)(p12p10;q10) der(9;10)(q10;p10) der(10)t(10;11)(q21;q14) der(13;16)(q10;q10) der(14)t(14;15)(?;?) der(14)t(14;15;1)(14?::15?::1?) dup(17)(q10) der(17)t(17;17;18)(17q10->q25::17q10->q23::18q21->q23) der(17)t(17;20;13)(17p13->q25::20?::13?) der(18)t(18;20)(p11.3;p11) der(18)t(18;22)(q21;q10) der(21)t(20;21)(?;?) der(?)t(5;7)(?;?) der(?)t(7;?;?)(7?::?::?) der(?)t(13;20;10;12)(13?::20?::10?::12?) der(?)t(16;17)(?;?) der(?)t(17;?)(?;?)
SqC-013	M/76	$T_2N_2M_0$	2n	Normal karyotype
SqC-015	F/69	$T_2N_0M_0$	2n	der(2;18)(p10;q10) der(6)t(6;7)(q10;p11.2) der(7)t(1;18;7)(1q21->q44::18?::7p22->q11.2) i(8)(q10) der(8;10)(q10;q10) der(14)t(1;14)(p13;q10) der(?)t(8;15)(?;?) der(?)t(15;8;10)(15?::8?::10?)
SqC-016	M/75	$T_2N_0M_0$	3n	der(X)t(X;2)(q11;?) der(X)t(X;6)(?;?) der(X)t(X;12)(q13;q15) der(X)t(X;15)(q22;q26) der(X)t(X;19)(?;?) der(1;13)(q10;q10) der(3)t(3;7)(p10;?) ins(3;10)(cen;?) der(3)t(3;10;3;12)(3p26->q10::10?::3p10->p21::12?) der(3;17)(q10;q10) t(4;18)(?;?) der(4)t(4;20)(?;?) der(15)t(6;15)(q13;q26) der(?)t(3;17)(?;?) der(?)t(8;9)(?;?)

(*continued on next page*)

Table 3 (*continued*)

Patient	Sex/age	TNM staging	Ploidy status	Clonal rearrangements
				der(?)t(9;13)(?;?) der(?)t(11;19)(?;?) der(?)t(13;19)(?;?) der(?)t(14;21)(?;?)
SqC-017	M/53	$T_2N_0M_0$	2n	Normal karyotype
SqC-029	M/70	$T_3N_1M_0$	2n	Normal karyotype
SqC-030	M/83	$T_2N_1M_0$	2n	Normal karyotype
SqC-031	M/78	$T_1N_0M_0$	2n	Normal karyotype
SqC-032	M/62	$T_1N_0M_0$	2n	der(X)t(X;5)(?;p15) der(Y)t(Y;20;?;?)(Yp11.3->q12::20?::?::?) dup(1)(?) der(1;13)(p10;q10) der(4;6)(q10;p10) der(6)t(6;20)(q11;?) der(8)t(8;16)(?;p11) i(9)(q?) der(9)t(4;9)(q13;p21) der(15;20)(q10;q10) der(17)t(10;17)(?;p13) der(20)t(4;20)(?;p10) der(?)t(3:13)(?;?) der(?)t(6;8)(?;?)
SqC-033	M/80	$T_2N_0M_0$	3n	dic(X;16)(q13;p10) der(1)t(1;3)(q32;q26) der(1)t(1;5)(p13;p10) der(2;17)(p10;q10) der(4)t(4;2)(q25;q33) der(4)t(4;15)(q34;q22) der(5)t(5;22;6)(5p15.3->p10::22?::6?) der(13;15)(q10;q10) der(18)t(17;18)(q21;q10) der(19)t(5;19)(p10;q13.1) der(?)t(1;13)(?;?) der(?)t(2;1;15)(?;?;?) der(?)t(6;15)(?;?) der(?)t(7;8)(?;?) der(?)t(7;22)(?;?) der(?)t(8;15)(?;?) der(?)t(15;20)(?;?) der(?)t(18;15;6)(18?::15?::6?)
SqC-034	M/53	$T_2N_0M_0$	2n	Normal karyotype
SqC-035	M/62	$T_2N_0M_0$	2n	Normal karyotype
AdC-002	M/72	$T_4N_0M_0$	2n	der(15)t(10;15)(?;q26)
AdC-005	F/72	$T_2N_0M_0$	2n	Normal karyotype
AdC-006	M/60	$T_2N_0M_0$	2n	der(9)t(9;10)(q21;q23q25) der(5)t(5;7)(p15;p13) der(10)t(10;9;10)(10p15->q22::9q22->q34::10q26) der(10)t(10;?)(q23;?)
AdC-008	M/68	$T_2N_0M_0$	3n	der(X)t(X;17)(p11.2;q11.2) der(Y)t(Y;15;15)(Yp11.3->q12::15q11.2->q26::15q11.2->q26) der(2)t(2;12)(p11.2;q13) der(5;20)(q10;q10) i(6)(q10) der(6;11)(p10;q10) der(7;11)(p10;q10) i(8)(q10)

(*continued on next page*)

Table 3 (*continued*)

Patient	Sex/age	TNM staging	Ploidy status	Clonal rearrangements
				der(8)t(8;17)(q11.2;?) der(10;17)(q10;q10) der(10;15)(q10;q10) i(11)(p10) der(12;19)(q10;q10) dic(17)t(17;19)(q11.2;p13.2) der(20)t(3;20)(?;p11.2) der(?)t(9;16)(?;?)
AdC-009	M/68	$T_1N_0M_0$	2n	Normal karyotype
AdC-010	M/66	$T_2N_0M_0$	2n	Normal karyotype
AdC-011	M/68	$T_4N_0M_0$	2n	Normal karyotype
AdC-012	M/78	$T_2N_0M_0$	3n	i(1)(q10) ins(5;13)(q34;q?) der(6)t(5;6)(?;?) der(6)t(6;13;7)(6p25->q11::13q?::7q22->p22) der(11)t(11;13)(q10;q12) der(12)t(14;2;8;12;15)(14q?::2?::8?::12?::15q?) der(12)t(12;8;12)(12q10->q24.3::8?::12?) dic(12;17)t(17;8;12;15)(17p13->q25::8?::12p13->q22::15q?) der(14)t(14;21)(q10;q11.2) der(17)t(17;15;17;17)(17p13->p10::15?::17q21->q25::17q21->q25)
AdC-015	M/45	$T_2N_0M_0$	2n	t(4;7)(q25;?)
AdC-018	M/43	$T_2N_1M_0$	3n	i(X)(q10) der(1;14)(q10;q10) der(2;14)(q10;q10) der(5)t(5;19)(p15;?q13.1) dic(10;22)(p15;q13) i(13)(q10) der(17;20)(p10;q10) der(?)t(4;6)(?;?)
AdC-020	M/73	$T_2N_0M_0$	4n	der(Y)t(Y;21;12)(Yp11.3->q12::21?::12q13->q24.3) der(1)t(1;22;12)(1p13->q44::22?::12p11.2->p13) dic(4;20)(p10;p13) der(4)t(4;22)(?q33;q11) der(6)t(6;17)(p23;q21) der(9)t(8;9)(q11;q34)
AdC-021	M/72	$T_2N_0M_0$	3n	der(X)t(X;16;X)(Xp22.3->q13::16?::Xq24->q28) i(Y)(q10) der(Y)t(11;Y)(q21;p11) der(1)t(1;18)(p13;?) der(2;9)(q10;q10) der(4;12)(q10;q10) der(5)t(5;6)(q11;q13) der(5;8)(p10;p10) der(7)t(7;10)(p15;?) der(7)(q36p22;q11q36) der(8;14)(q10;q10) der(9)t(1;9)(p10;p13) der(9)t(9;16;1)(p10;?;?) der(12)t(7;12)(?;q22) der(14)t(11;14)(q?;q32) dic(16;19)t(19;1;16)(19q13.2->q13.3::1?::16p13.3->q24) der(19)t(11;19)(q22;q13.2) der(19;22)(p10;q10)
AdC-022	M/43	$T_4N_0M_0$	2n	der(X)t(X;12)(p22;?) der(5)t(5;16)(p11;?)
AdC-024	M/68	$T_2N_0M_0$	3n	der(X)t(X;11)(?;q?)

(*continued on next page*)

Table 3 (*continued*)

Patient	Sex/age	TNM staging	Ploidy status	Clonal rearrangements
				der(X)t(X;16)(?:p13.3) der(4)t(4;20)(?;?) der(4)t(4;15;2)(4?::15q12->q26::2?) der(8)t(8;15)(q10;?) der(8)t(8;15;2)(8?::15q12->q26::2?) ins(12;16)(p11;?) der(13)t(6;13)(p10;q10) der(14)t(6;14)(?;q10) der(17)t(3;17)(?;p13)
AdC-025	M/68	$T_1N_0M_0$	2n	der(2)t(2;?9)(q33;?) der(4)t(14;4;9;22)(14?::4p11->q21::9q?::22q11.2->q13) der(4)t(4;12;8)(4p16->q35::12?::8q22->q24.3) der(6;7)(q10;q10) ins(20;8)(20p13->p10::8q11.2-> q23::20q11.2->q13) der(20)t(20;8;20;8;20)(20q13->q11.2::8q11.2->q23::20p10->p13::8q11.2->q23::20q11.2->q13) der(22)t(21;22)(q10;q13)
AdC-026	M/48	$T_1N_0M_0$	2n	der(16)t(12;16)(?p10;p10)
AdC-027	M/75	$T_2N_1M_1$	2n	der(1)t(1;21)(q42;?) der(7)t(7;22)(p22;q13)
AdC-028	M/71	$T_2N_0M_0$	2n	del(8)(q13) der(12)t(8;12)(q24.1;q21)
AdC-033	M/71	$T_3N_2M_0$	4n	der(X)t(X;11)(q22;p15) der(X)t(X;11;19)(Xp22.3->?p21::11q?::19q13.2->q13.3) dic(Y;1)t(Y;1;8)(Yp11.3->q12::1q10->q32::8q21->q24) der(1)t(14;1;8)(14q32->q11.2::1q10->q32::8q21->q24) der(1)t(1;13)(p10;?) der(2)t(2;13)(q10;q10) dic(1;4)t(4;1;8)(4p16->q35::1q10->q32::8q21->q24) dup(4)(q22q35) ins(6;8)(p22;?) der(8)t(8;14;7)(8p11->q11::14q11.2->q32::7q21->q36) der(14)t(14;7;2)(14q10->q?24::7q?::2?) i(17)(q10) der(19)t(18;19)(p10:q13.1) der(?)t(17;22)(?;?)
AdC-034	M/69	$T_2N_2M_0$	2n	der(3)t(3;19)(q10;q13.1)

Hierarchical clustering was simulated from our CGH findings, revealing two major cluster dendrograms that represent the patterns of genetic alteration associated with SqC and AdC (Fig. 1). Our finding supports the notion that the two histological subtypes progress through differing pathogenetic pathways and further indicates that SqC and AdC can be readily distinguished from each other at the chromosomal level. Specific copy-number gains that were significantly higher in SqC than AdC included 2p13-p11.2, 3q25-q29, 6p21.2-p12, 9q13-q34, 12p, 12q12-q15, and 17q21 ($P<0.05$). Copy-number losses on regional 3p, 4q, 8p, 9p and 13q were also more frequently observed in SqC ($P<0.05$) (Table 2). Notably, a small series of AdC characterised by common Xq13-q28 over-representations was found clustered into a sub-branch under the SqC dendrogram. Previous expression profiling of NSCLC also showed an AdC subgroup within the SqC transcriptional pattern [26]. A summary of CGH findings is displayed in Fig. 2. Our current CGH clustering concurs with the earlier report and points to Xq13-q28 as one of the features that could further assist in classifying AdC patient subgroups. In contrast, further statistical correlations among TNM stages in both the AdC and SqC series did not yield significant genetic changes in association with tumour progression.

The high percentage incidence of +3q25-q29 (85.7%), +17q21 (53.57%), +9q13-q34 (32.14%) and loss of 13q (28.57%) detected in our present SqC series could represent specific tumour-progression pathways that promote the development of SqC. Amplification of chromosome 3q has been described in SqC of different

origins, such as lung, oral and vulvar [27,28]. Although a 3q gain might have a role in the early stages of SqC of the uterine cervix and head and neck [29,30], recent studies have also shown a positive correlation between 3q over-representation and the invasiveness and progress of oral, oesophageal and hypopharyngeal cancers [31–33]. Positional mapping by array-based CGH analysis on the 3q amplicon in SqC of the lung has implicated *PIK3CA* as one putative oncogene [34]. Genomic amplification of other genes within the same region, such as *BCHE* and *SLC2A2* (both on 3q26), has also been confirmed in SqC by F*IS*H analysis [35].

It is well known that varying degrees of keratinisation are a characteristic of SqC. Recent expression profiling has suggested that there is frequent upregulation of cytokeratin overexpression in SqC. Type I cytokeratins *KRT10, 13, 14, 15, 16,* 19, 20 and *KRT23*, located at 17q21, might be involved,in the keratinisation of SqC [36]. The frequent loss of 13q21 and the proximal translocations detected in the present series might influence the perturbation of the putative tumour-suppressor *BRCA2* gene (on 13q21). Deletion of the *BRCA2* gene results in the loss of genes that regulate the cell-cycle, enabling proliferation and tumorigenesis [37]. BRCA2

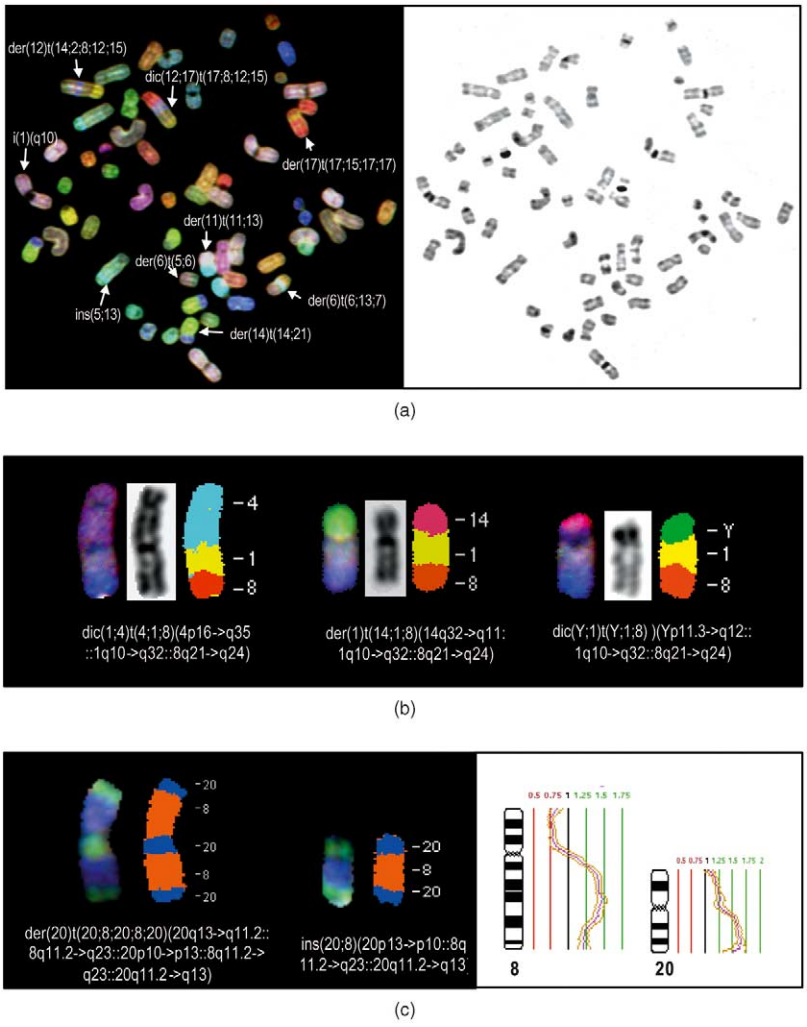

Fig. 3. Spectral karyotyping (SKY) analysis of primary non-small cell lung cancers. (a) Hybridised spectral image and corresponding reverse 4′,6-diamidino-2-phenylindole (DAPI) image of a primary adenocarcinoma. SKY analysis shows the presence of frequent non-reciprocal translocations. Simple and complex interchromosomal translocations of i(1)(q10), ins(5;13)(q34;q?), der(6)t(5;6)(?;?), der(6)t(6;13;7)(6p25->q11::13q?::7q22->p22), der(11)t(11;13)(q10;q12), der(14)t(14;21)(q10;q11.2), der(17)t(17;15;17;17)(17p13->p10::15?::17q21->q25::17q21->q25), der(12)t(14;2;8;12;15)(14q?::2?::8?::12?::15q?) and dic(12;17)t(17;8;12;15)(17p13->q25::8?::12p13->q22::15q?) are suggested. (b) Clonal occurrence of translocation pair in a case of adenocarcinoma. Derivative core of chromosomes 1 and 8 is shown with complex chromosomal rearrangements. Spectral image, reverse DAPI image together with the classified image show the derivative core t(1;8) in rearrangement with third-party chromosomes, dic(1;4)t(4;1;8), der(1)t(14;1;8) and dic(Y;1)t(Y;1;8). Identical reverse DAPI bandings of t(1;8)(1q10->q32::8q21->q24) are visible among these translocated chromosomes. (c) Chromosomal coamplification corresponding to translocation partnership. Comparative genomic hybridisation shows 8p loss, 8q11.2-q23 amplification, 20p low-level gain and 20q amplification in a case of adenocarcinoma. Corresponding SKY examination reveals a complex derivative of chromosomes 8 and 20, der(20)t(20;8;20;8;20). A translocation intermediate ins(20;8) was also captured. The spectral and classified images of derivative chromosomes are shown.

protein is also associated with the activation of double-strand break (DSB) repair via homologous recombination. Since chromosomal instability could occur as a consequence of the disruption of DNA repair or recombination pathways [38], it is possible that the gross chromosomal alterations detected in SqC may be related to defective DSB repair mechanisms caused by an abnormality in the BRCA pathway.

3.2. Chromosomal coamplification and translocation partnership

SKY analysis of 41 informative cases (21 SqC, 20 AdC) showed the frequent presence of non-reciprocal translocations. Clonal rearrangements in individual cases as determined by SKY are summarised in Table 3. An example of the suggested complex karyotype is shown in Fig. 3(a). In addition, the manifestation of complex rearrangements as translocation families was also found. In several patients with complex karyotypes, derivative chromosomes appeared to share a common translocated chromosome pair, i.e. differed only by a further translocation with a third-party chromosome. The parts of the derivative core, which was never captured as a 'stand alone' simple translocation, shared exactly the same inverted DAPI bandings. All complex rearrangements within a translocation family were found to be clonal and are therefore likely to be replicas of the same ancestral core. Examples of translocation partners are illustrated in Fig. 3(b).

Several groups of translocation partners involving chromosome 8q gain were common in SqC and AdC; these included t(7;8), t(8;15), and t(8;9). In particular, the translocation partnership between chromosomes 8q and 12q, t(8;12)(q21∼q22;q22∼q24) was exclusive to the AdC series. Other translocation partners detected, though less frequent than chromosome 8q, included t(1;13), t(1;15), t(2;17) and t(15;20). The occurrence of translocation partners was further suggested in cases that displayed genomic amplifications on the concordant regions in CGH analyses (Fig. 3c). Using a mouse model, it has been demonstrated that translocation can lead to the simultaneous amplification of oncogenic sequences in juxtaposition within a complex rearrangement [39]. The acquired translocation partnership observed here might thus have implications for structural stability and the provision of clonal advantages to the transformed SqC and AdC cells.

This study is a comprehensive investigation into cytogenetic alterations in primary NSCLC. Structural changes encompassed by clonal rearrangement and marker chromosomes of uncertain origin, which would otherwise have been difficult to be elucidated by conventional G-banding, were clarified by SKY. Based on the findings from CGH and SKY analyses, the recurrent aberrant sites detected have emphasised the areas where a dosage modification of oncogene or tumour-suppressor genes might have occurred. Future studies on defining the genes involved may thus be of value in understanding the carcinogenesis of NSCLC.

Acknowledgements

This work was supported by a grant from the Research Grants Council of Hong Kong (Ref. No.: CUHK 4112/00M), and by The Kadoorie Charitable Foundations (under the auspices of the Hong Kong Cancer Genetics Research Group).

References

1. Jemal A, Thomas A, Murray T, Thun M. Cancer Statistics, 2002. *CA Cancer J Clin* 2002, **52**, 23–47.
2. Wynder EL, Goodman MT, Hoffmann D. Lung cancer etiology: challenges of the future. *Carcinog Compr Surv* 1985, **8**, 39–62.
3. Wang T-J, Zhou B-S. Meta-analysis of the potential relationship between exposure to environmental tobacco smoke and lung cancer in nonsmoking Chinese women. *Lung Cancer* 1997, **16**, 145–150.
4. Luk C, Tsao M-S, Bayani J, Shepherd F, Squire JA. Molecular cytogenetic analysis of non-small cell lung carcinoma by spectral karyotyping and comparative genomic hybridization. *Cancer Genetics and Cytogenetics* 2001, **125**, 87–99.
5. Petersen I, Bujard M, Petersen S, *et al*. Patterns of chromosomal imbalances in adenocarcinoma and squamous cell carcinoma of the lung. *Cancer Res* 1997, **57**, 2331–2335.
6. Pei J, Balsara BR, Li W, *et al*. Genomic imbalances in human lung adenocarcinomas and squamous cell carcinomas. *Genes, Chromosomes & Cancer* 2001, **31**, 282–287.
7. Luk C, Tsao MS, Bayani J, Shepherd F, Squire JA. Molecular cytogenetic analysis of non-small cell lung carcinoma by spectral karyotyping and comparative genomic hybridization. *Cancer Genet Cytogenet* 2001, **125**, 87–99.
8. Speicher MR, Petersen S, Uhrig S, *et al*. Analysis of chromosomal alterations in non-small cell lung cancer by multiplex-FISH, comparative genomic hybridization, and multicolor bar coding. *Lab Invest* 2000, **80**, 1031–1041.
9. Kallioniemi AKO-P, Sudar D, Rudovitz D, Gray JW, Waldman F, Pinkle D. Comparavtive genomic hybridization for molecular cytogenetic analysis of solid tumors. *Science* 1992, **258**, 818–821.
10. Wong NLP, Lee SW, Fan S, *et al*. Assessment of genetic changes in hepatocellular carcinoma by comparative genomic hybridization analysis. *Am J Pathol* 1999, **154**, 37–43.
11. du Manoir S, Schrock E, Bentz M, *et al*. Quantitative analysis of comparative genomic hybridization. *Cytometry* 1995, **19**, 27–41.
12. du Manoir S, Kallioniemi OP, Lichter P, *et al*. Hardware and software requirements for quantitative analysis of comparative genomic hybridization. *Cytometry* 1995, **19**, 4–9.
13. Eisen MB, Spellman PT, Brown PO, Botstein D. Cluster analysis and display of genome-wide expression patterns. *PNAS* 1998, **95**, 14863–14868.
14. Wong N, Lai P, Pang E, Leung TW, Lau JW, Johnson PJ. A comprehensive karyotypic study on human hepatocellular carcinoma by spectral karyotyping. *Hepatology* 2000, **32**, 1060–1068.
15. Schrock EDMS, Veldman T, Schoell B, *et al*. Multicolor spectral karyotyping of human chromosomes [Reports]. *Science* 1996, **273**, 494–497.

16. Mitelman F. *ISCN (1995): An International System for Human Cytogenetic Nomenclature*. Basel, S. Karger Publishers, Inc, 1995.
17. Kubokura H, Tenjin T, Akiyama H, *et al*. Relations of the c-myc gene and chromosome 8 in non-small cell lung cancer: analysis by fluorescence in situ hybridization. *Ann Thorac Cardiovasc Surg* 2001, **7**, 197–203.
18. Wang J, Xie LY, Allan S, Beach D, Hannon GJ. Myc activates telomerase. *Genes Dev* 1998, **12**, 1769–1774.
19. Counter CM, Hahn WC, Wei W, *et al*. Dissociation among in vitro telomerase activity, telomere maintenance, and cellular immortalization. *PNAS* 1998, **95**, 14723–14728.
20. Halvorsen TL, Leibowitz G, Levine F. Telomerase activity is sufficient to allow transformed cells to escape from crisis. *Mol Cell Biol* 1999, **19**, 1864–1870.
21. Fujita Y, Fujikane T, Fujiuchi S, *et al*. The diagnostic and prognostic relevance of human telomerase reverse transcriptase mRNA expression detected in situ in patients with nonsmall cell lung carcinoma. *Cancer* 2003, **98**, 1008–1013.
22. Sozzi G, Conte D, Leon M, *et al*. Quantification of free circulating DNA as a diagnostic marker in lung cancer. *J Clin Oncol*, 2003.
23. Kanamoto T, Hellman U, Heldin CH, Souchelnytskyi S. Functional proteomics of transforming growth factor-beta1-stimulated Mv1Lu epithelial cells: Rad51 as a target of TGFbeta1-dependent regulation of DNA repair. *Embo J* 2002, **21**, 1219–1230.
24. Vafa O, Wade M, Kern S, *et al*. c-Myc can induce DNA damage, increase reactive oxygen species, and mitigate p53 function: a mechanism for oncogene-induced genetic instability. *Mol Cell* 2002, **9**, 1031–1044.
25. Cairns J. Somatic stem cells and the kinetics of mutagenesis and carcinogenesis. *Proc Natl Acad Sci USA* 2002, **99**, 10567–10570.
26. Bhattacharjee A, Richards WG, Staunton J, *et al*. Classification of human lung carcinomas by mRNA expression profiling reveals distinct adenocarcinoma subclasses. *Proc Natl Acad Sci USA* 2001, **98**, 1375–1379.
27. Allen DG, Hutchins AM, Hammet F, *et al*. Genetic aberrations detected by comparative genomic hybridisation in vulvar cancers. *Br J Cancer* 2002, **86**, 924–928.
28. Ashman JN, Patmore HS, Condon LT, Cawkwell L, Stafford ND, Greenman J. Prognostic value of genomic alterations in head and neck squamous cell carcinoma detected by comparative genomic hybridisation. *Br J Cancer* 2003, **89**, 864–869.
29. Umayahara K, Numa F, Suehiro Y, *et al*. Comparative genomic hybridization detects genetic alterations during early stages of cervical cancer progression. *Genes Chromosomes Cancer* 2002, **33**, 98–102.
30. Redon R, Muller D, Caulee K, Wanherdrick K, Abecassis J, du Manoir S. A simple specific pattern of chromosomal aberrations at early stages of head and neck squamous cell carcinomas: PIK3CA but not p63 gene as a likely target of 3q26-qter gains. *Cancer Res* 2001, **61**, 4122–4129.
31. Oga A, Kong G, Tae K, Lee Y, Sasaki K. Comparative genomic hybridization analysis reveals 3q gain resulting in genetic alteration in 3q in advanced oral squamous cell carcinoma. *Cancer Genet Cytogenet* 2001, **127**, 24–29.
32. Noguchi T, Kimura Y, Takeno S, *et al*. Chromosomal imbalance in esophageal squamous cell carcinoma: 3q gain correlates with tumor progression but not prognostic significance. *Oncol Rep* 2003, **10**, 1393–1400.
33. Steinhart H, Bohlender JE, Constantinidis J, *et al*. Genetic imbalances in preinvasive tissue of hypopharynx provide evidence for cytogenetic heterogeneity. *Oncol Rep* 2001, **8**, 1229–1231.
34. Massion PP, Kuo W-L, Stokoe D, *et al*. Genomic copy number analysis of non-small cell lung cancer using array comparative genomic hybridization: implications of the phosphatidylinositol 3-kinase pathway. *Cancer Res* 2002, **62**, 3636–3640.
35. Brass N, Racz A, Heckel D, Remberger K, Sybrecht GW, Meese EU. Amplification of the genes BCHE and SLC2A2 in 40% of squamous cell carcinoma of the lung. *Cancer Res* 1997, **57**, 2290–2294.
36. Virtanen C, Ishikawa Y, Honjoh D, *et al*. Integrated classification of lung tumors and cell lines by expression profiling. *PNAS* 2002, **99**, 12357–12362.
37. Tutt A, Gabriel A, Bertwistle D, *et al*. Absence of Brca2 causes genome instability by chromosome breakage and loss associated with centrosome amplification. *Curr Biol* 1999, **9**, 1107–1110.
38. Venkitaraman AR. Cancer susceptibility and the functions of BRCA1 and BRCA2. *Cell* 2002, **108**, 171–182.
39. Zhu C, Mills KD, Ferguson DO, *et al*. Unrepaired DNA breaks in p53-deficient cells lead to oncogenic gene amplification subsequent to translocations. *Cell* 2002, **109**, 811–821.